The oxazolidinone antibiotics perturb the ribosomal peptidyl-transferase center and effect tRNA positioning

Daniel N. Wilson*[†‡§], Frank Schluenzen[‡¶], Joerg M. Harms[‡‖], Agata L. Starosta*, Sean R. Connell[‖], and Paola Fucini[§‖]

*Gene Center and Department of Chemistry and Biochemistry and [†]Munich Centre for Integrated Protein Science, University of Munich, Feodor Lynen Strasse 25, 81377 Munich, Germany; [¶]Deutsches Elektronen-Synchrotron, Notkestrasse 85, D-22603 Hamburg, Germany; and [‖]Cluster of Excellence for Macromolecular Complexes, Institut für Organische Chemie und Chemische Biologie, Johann Wolfgang Goethe-Universität, Max-von-Laue-Strasse 7, D-60438 Frankfurt am Main, Germany

Edited by V. Ramakrishnan, Medical Research Council, Cambridge, United Kingdom, and approved June 25, 2008 (received for review May 2, 2008)

The oxazolidinones represent the first new class of antibiotics to enter into clinical usage within the past 30 years, but their binding site and mechanism of action has not been fully characterized. We have determined the crystal structure of the oxazolidinone linezolid bound to the *Deinococcus radiodurans* 50S ribosomal subunit. Linezolid binds in the A site pocket at the peptidyltransferase center of the ribosome overlapping the aminoacyl moiety of an A-site bound tRNA as well as many clinically important antibiotics. Binding of linezolid stabilizes a distinct conformation of the universally conserved 23S rRNA nucleotide U2585 that would be nonproductive for peptide bond formation. In conjunction with available biochemical data, we present a model whereby oxazolidinones impart their inhibitory effect by perturbing the correct positioning of tRNAs on the ribosome.

ribosome | translation | linezolid

Protein synthesis in all living cells occurs on macromolecular complexes called ribosomes. The active site for amino acid polymerization is located in a cleft on the interface side of the large ribosomal subunit, referred to as the peptidyltransferase center (PTC). The importance of this functional center is illustrated by the fact that the ribosome is one of the major targets within the cell for antimicrobials, many of which execute their inhibitory effect by binding at the PTC (reviewed in refs. 1 and 2). In the past seven years crystal structures have appeared for almost every major class of antibiotics that target the ribosome, including those that bind at the PTC, such as anisomycin (3), the streptogramins (4, 5), chloramphenicols (6), lincosomides such as clindamycin (5, 6), and the pleuromutilins, for example tiamulin (7). Despite this extensive work, the structure of a ribosome in complex with the clinically important oxazolidinone class of drugs has so far not been reported in the literature.

The first oxazolidinone to enter into the market was linezolid, launched in 2000 under the tradename Zyvox by Amersham Pharmacia (now Pfizer). This represented a landmark in antimicrobial research with linezolid being the first truly new class of antibiotic to pass clinical trials in 20 years. Since then, oxazolidinones have been shown to be very potent in the ongoing battle against multidrug-resistant bacteria, displaying activity against a variety of Gram-positive and, more recently, Gram-negative pathogens. In particular, oxazolidinones are used to treat skin and respiratory tract infections caused by *Staphlococcus aureus* and *Streptococci* strains, as well as being active against vancomycin-resistant *Enterococcus faecium* (reviewed in refs. 8–10).

In vitro cross-linking and footprinting studies to determine the site of interaction on the ribosome suggest that the oxazolidinones bind in the vicinity of the L1 stalk but also bind to the small subunit (11). In contrast, recent studies using an elegant *in vivo* cross-linking approach revealed the PTC as the *bone fide* drug target (12, 13). These latter studies are consistent with the observation that drug resistance in both archaea and bacteria arises through mutation of nucleotides located within the PTC [Fig. 1*A* and supporting information (SI) Fig. S1] (14–19). Although translation is recognized as the main target of oxazolidinones, there still remains some controversy as to the step of inhibition. Oxazolidinones have been suggested to inhibit translational events ranging from initiation and the formation of the first peptide bond, EF-G dependent translocation during elongation and frameshifting, to non-sense suppression during termination (for example, see refs. 11 and 19–22).

Here we have determined the crystal structure of the oxazolidinone linezolid bound to the eubacterial *Deinococcus radiodurans* 50S ribosomal subunit at 3.5 Å and show unambiguously that the drug binds within the PTC of the ribosome. The binding position of linezolid overlaps with the aminoacyl moiety of an A-site bound tRNA, as well as many drugs that inhibit A-site action, such as chloramphenicol and anisomycin. Binding of linezolid stabilizes the nucleobase of U2585 (*Escherichia coli* numbering used throughout) in an orientation that is distinctly different from when A and P-site tRNA ligands are bound, suggesting that linezolid induces a nonproductive conformation of the PTC. Taken together with the available biochemical data on oxazolidinone action, we present a model for the mechanism of action of this clinically important class of antibiotics.

Results

The Binding Position of Linezolid on the Ribosome. Crystals of the native *D. radiodurans* large ribosomal subunit (D50S) were soaked for 2 h in a solution containing physiologically relevant concentrations (5 μM) of linezolid; $\approx$2 μM and $\approx$10 μM have been shown to inhibit *E. coli in-vitro*-coupled transcription–translation assays by 50% and 90%, respectively (23). The linezolid-treated crystals yielded diffraction data to a resolution of 3.3 Å (Table S1). Additional electron density is clearly observable within the PTC that is not present within the equivalent region of D50S native maps (Fig. S2) and was therefore attributed to the drug (Fig. 1*B*). Linezolid comprises

BIOCHEMISTRY

Author contributions: D.N.W., F.S., and P.F. designed research; D.N.W., F.S., and J.M.H. performed research; D.N.W., F.S., J.M.H., A.L.S., S.R.C., and P.F. analyzed data; and D.N.W., F.S., S.R.C., and P.F. wrote the paper.

The authors declare no conflict of interest.

This article is a PNAS Direct Submission.

Data deposition: The coordinates and structure factors reported in this paper have been deposited in the Protein Data Bank, www.pdb.org (PDB ID code 3DLL).

[‡]D.N.W., F.S., and J.M.H. contributed equally to this work.

[§]To whom correspondence may be addressed. E-mail: wilson@lmb.uni-muenchen.de or fucini@chemie.uni-frankfurt.de.

This article contains supporting information online at www.pnas.org/cgi/content/full/0804276105/DCSupplemental.

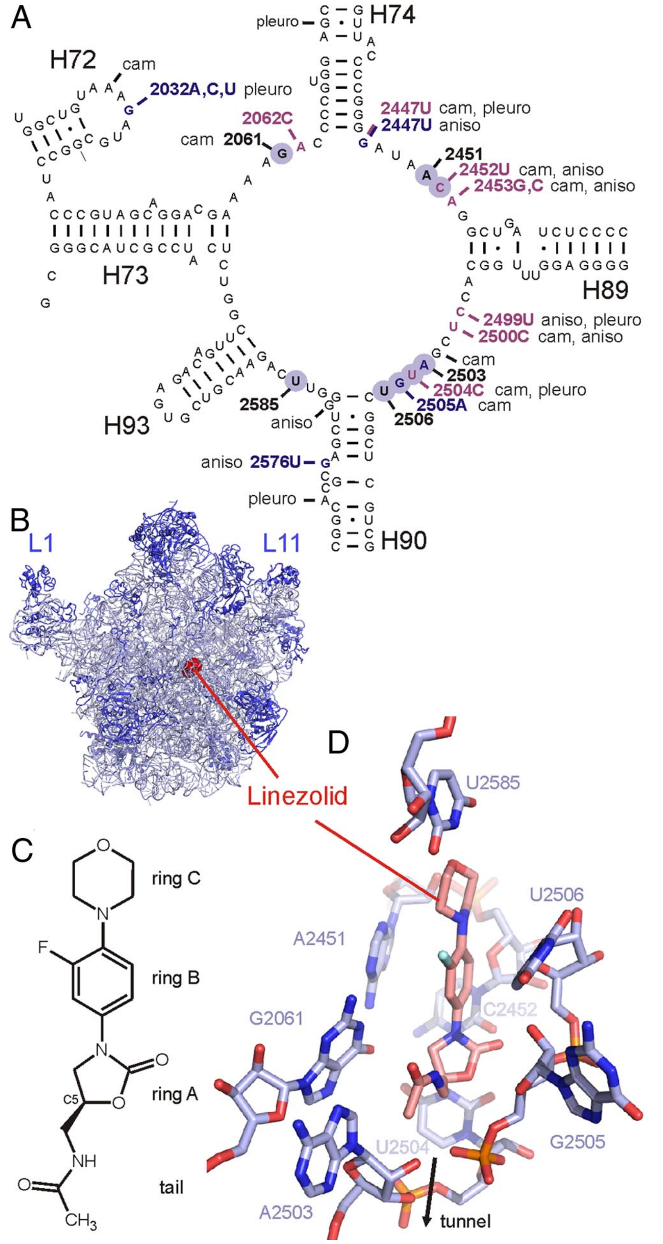

Fig. 1. The binding site of oxazolidinones. (*A*) Secondary structure of the peptidyltransferase ring of the 23S rRNA from *D. radiodurans* with the mutation sites in bacteria (blue) and archaea (purple) that confer resistance to oxazolidinones indicated with *E. coli* numbering. Nucleotides that directly interact with linezolid are shaded light blue, and the mutations sites associated with resistance for chloramphenicol (cam) (45, 46), anisomycin (aniso) (47, 48), and pleuromutilins (pleuro) (49) are shown. (*B*) Interface view of the *D. radiodurans* 50S subunit with the binding position of linezolid (red) and landmark proteins L1 and L11 as indicated. (*C*) Chemical structure of linezolid, highlighting the three aromatic rings (*A–C*) and the acetamidomethyl tail. (*D*) View of linezolid (pink) within the binding pocket formed by eight universally conserved nucleotides (blue) of the 23S rRNA. The arrow indicates tunnel direction.

four chemical moieties, namely three aromatic rings and an acetamidomethyl tail (Fig. 1*C*). Ring-A represents the pharmacokinetic oxazolidinone ring from which this class of antimicrobials derive their name. Linezolid binds at the PTC within a pocket composed of universally conserved residues (Fig. 1*D* and Fig. S1) and is located such that ring-C orients toward the intersubunit interface, whereas ring-A as well as the C5-tail head in the general direction of the ribosomal tunnel. Within the pocket, the oxazolidinone ring stacks on U2504 (although the geometry and distance are not optimal for Pi-orbital stacking), and the C5-tail extends toward A2503 (Fig. 1*D*). Ring-B is sandwiched between A2451 and U2506, and has been modeled with the C2 fluorine pointing out of the pocket for two reasons: (*i*) strong electron density is observed where the electron-rich fluorine atom would be located, and (*ii*) the fluorine atom can only contribute to the coordination of a putative magnesium ion that appears upon linezolid binding in this particular configuration (Fig. S2).

With the exception of U2585 (see the following section), no significant conformational change in the RNA forming the binding pocket is observable upon binding of linezolid (Fig. 2*A*). Indeed, the conformation of the majority of these nucleotides is almost identical in the empty *E. coli* 70S (24), fully refined *Haloarcula marismortui* 50S (25) as well as the recent high-resolution *Thermus thermophilus* 70S·mRNA·tRNA$_3$ structure (26). One obvious exception is the conformationally flexible U2506 nucleotide, which in the *T. thermophilus* 70S structure encroaches on the linezolid binding position, whereas in the *E. coli* and *H. marismortui* structures is oriented away from the drug (Fig. 2*A*). This base undergoes conformational change during the proper binding of tRNA ligands at the A site (27); therefore, restricting the flexibility of this base may also be important for the binding and inhibitory mechanism of oxazolidinones.

Although the overall position of linezolid on the *D. radiodurans* 50S subunit is similar to that of a structure of the same drug bound to *H. marismortui* 50S subunit (U.S. patent number 6,947,845 B2) as well as a biochemically deduced model for the drug bound to *E. coli* ribosome (13), the specifics in terms of ring orientations and interactions within the binding pocket appear to differ (Fig. 2 *B* and *C*). Nevertheless, the binding position for linezolid determined here on the *D. radiodurans* 50S subunit is consistent with the various cross-links observed from photoreactive oxazolidinone derivatives on the *E. coli* ribosome (Fig. S3 *a–c*).

Conformational Flexibility in U2585 Permits Different Oxazolidinone Binding Modes. In the native D50S structure, U2585 appears to be highly flexible and little density is visible for the nucleobase, even at low thresholds (Fig. S2), consistent with the multiple distinct positions this nucleotide adopts in the different ribosome structures (Fig. 3*A*). Upon binding of linezolid, however, stronger density for the base is observed (Fig. S2), suggesting that linezolid stabilizes U2585 through direct interaction. This may involve hydrogen-bonding because the N3 of U2585 is within hydrogen-bonding distance of the O4 of ring C of linezolid (Fig. 3*B*). What is perhaps most surprising is that this relatively weak hydrogen bond appears to be the sole hydrogen bond interaction that can form between the drug and RNA, thus relegating the majority of the contacts between linezolid and nucleotides within the PTC pocket to less energy-rich van der Waals and hydrophobic interactions.

Interestingly, modeling studies suggest that U2585 must adopt distinct positions to accommodate different oxazolidinone derivatives. A variety of different modes of interaction with the ring C attachments are observed, for example, a slight shift in U2585 enables hydrogen-bonding to the O1 of the furan ring of the clinical phase II drug, ranbezolid, whereas for an active tricyclic analog, U2585 can stack nicely on the aromatic fluorophenyl (ring D) side chain (Fig. S3 *d–f*). The flexibility of U2585 is important for the induced fit of P-tRNA binding at the PTC (27) and the binding of tRNA mimics to the PTC is impaired by mutation of U2585 (28). Therefore, the nonproductive conformation of U2585 for peptide bond formation may contribute to the inhibitory action of linezolid, analogous to the effect ob-

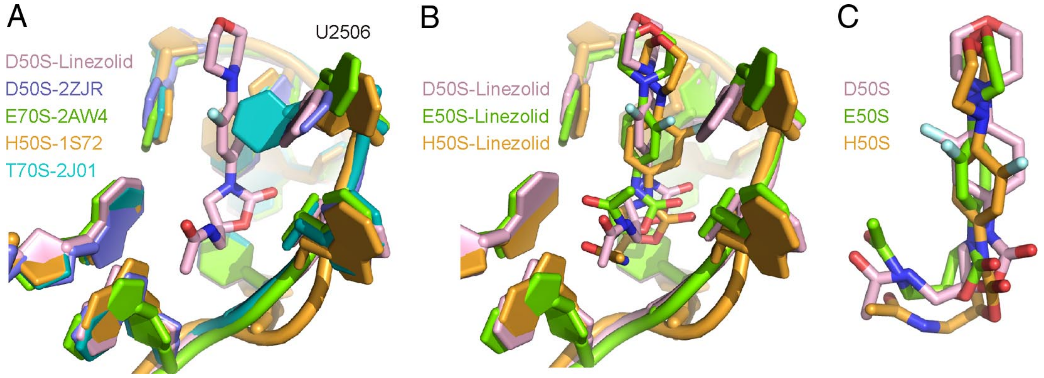

Fig. 2. Comparison of the linezolid binding pocket. (*A*) Comparison of linezolid binding pocket from the native D50S structure (PDB ID code 2ZJR; blue) with the D50S-linezolid structure (pink), as well as the native *E. coli* 70S (E70S; PDB ID code 2AW4; green) (24), the fully refined *H. marismortui* 50S (H50S; PDB ID code 1S72; orange) (25) and *T. thermophilus* 70S (T70S; PDB ID code 2J01; teal) (26). (*B*) Comparison of linezolid binding pocket on D50S (pink), with the model for bound to *E. coli* 70S (green) (13) and the *H. marismortui* 50S structure (orange; U.S. patent number6,947,845 B2). (*C*) Comparison of the position and orientation of linezolid from structures in *B*.

served when U2585 shifts upon streptogramin B binding at the PTC (Fig. S3*g*) (4).

Resistance to Oxazolidinones in Prokaryotes and Eukaryotes. All of the nucleotides that form the linezolid binding site are universally conserved (Fig. S1) and in many cases have been shown to be functionally important for the peptidyltransferase or peptidyl-tRNA hydrolysis activity of the ribosome (27, 29). Of these eight nucleotides, resistance mutations at only three of these positions, namely C2452U and U2504C in archaea and G2505A in eubacteria, have been reported (Fig. 1*A* and Fig. S1). Although the majority of the mutations that confer linezolid resistance are at nucleotides that do not directly interact with the drug, all of the mutation sites are located in nucleotides that lie adjacent to at least one of the universally conserved residues comprising the linezolid binding site. With the exception of G2576, which stacks directly onto G2505, all of the remaining mutation sites are clustered around G2504 and its base-pairing partner C2452 (Fig. 3*C*). In the D50S-linezolid structure, the oxazolidinone ring of the drug appears to stack against the base of U2504 and therefore it is easy to envisage how mutations at neighboring bases could confer resistance allosterically, probably by perturbing the positioning of U2504. It seems unlikely that the U2504 = C2452 base pair *per se* is important for linezolid binding, because, although it is present in all of the available bacterial ribosome structures, the base pair is absent in the *H. marismortui* 50S structures (despite both bases being conserved) due to a shifted position of U2504 (Fig. S4*a*). Generally, archaeal ribosomes are considered more ‘‘eukaryotic-like’’ with respect to their antibiotic specificities; however, this is not the case for the oxazolidinones as they have been shown to bind and/or inhibit both archaeal and bacterial (including mitochondrial) ribosomes but not to interact with human cytoplasmic ribosomes (13, 14). In the H50S-linezolid structure (U.S. patent number 6,947,845 B2), the drug appears to bind deeper in the binding pocket when compared with the position in D50S, which could result from the shifted position of U2504. Compared to linezolid, the shifted position of U2504 appears to have an even greater consequence for the binding of anisomycin to ribosomes, because the bacterial location of U2504 is incompatible with the binding position of anisomycin in the H50S structure (Fig. S4*b*), which is consistent with the susceptibility of archaeal ribosomes and the resistance exhibited by bacterial ribosomes to anisomycin (3, 30). In the absence of a crystal structure of a eukaryotic ribosome, we can only speculate about the innate resistance of these particles to linezolid, however, as noted previously (13), of the 10 mutations known to give rise to linezolid resistance in bacteria and archaea, the nucleotides corresponding to two of these mutations G2032C and C2499U are already present in the 28S rRNA (C4003 and U4562, respectively) of *Homo sapiens* (Fig. S1).

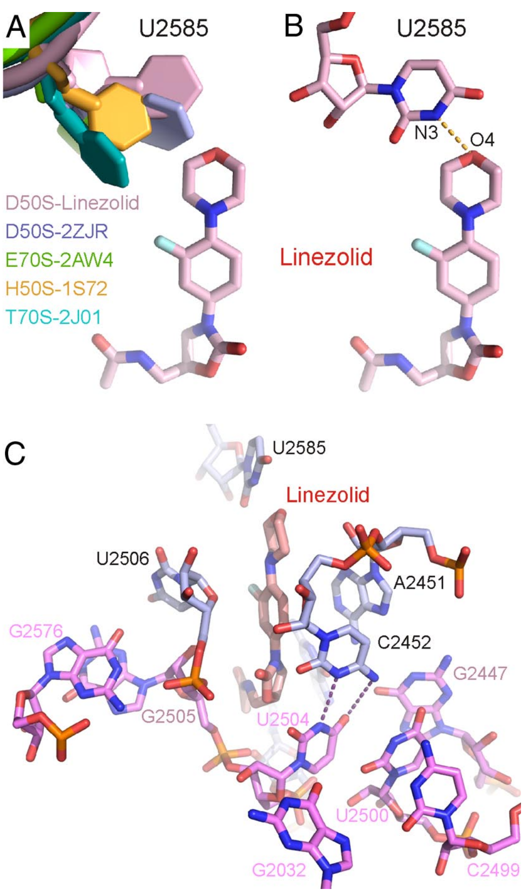

Fig. 3. Binding modes of U2585 and resistance to oxazolidinones. (*A*) Comparison of the position of U2585 between native (blue) and linezolid-bound (pink) D50S with E70S (green), H50S (orange), and T70S (teal) structures (PDB ID codes as in Fig. 2*A*). (*B*) Potential hydrogen bond (dashed line) between N3 of U2585 and O4 of ring-C of linezolid. (*C*) Overview of linezolid (pink) within the binding pocket, with sites of mutation that give rise to oxazolidinone resistance indicated in magenta. Dashed lines indicate hydrogen bonds between U2504 and C2452.

BIOCHEMISTRY

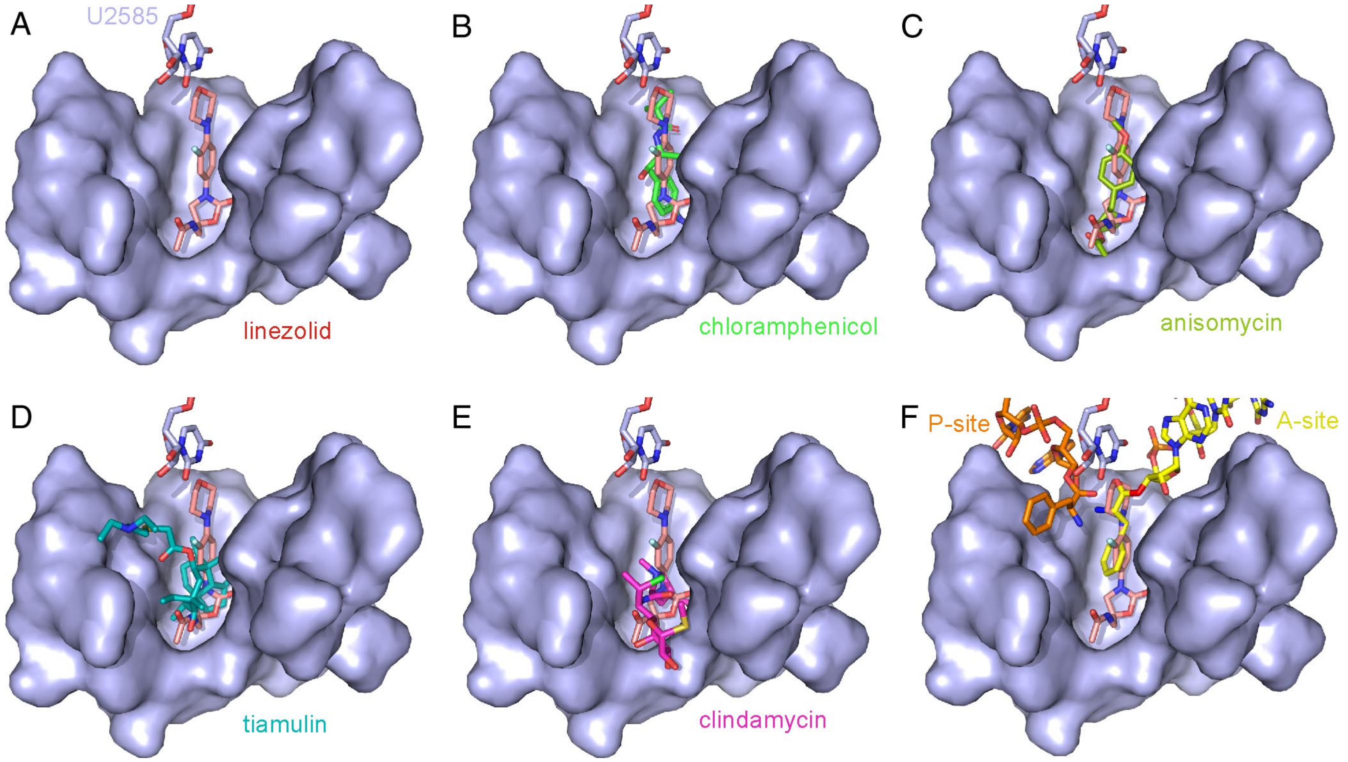

Fig. 4. Linezolid overlaps A-site ligands at the peptidyltransferase center. (*A–F*) Comparison of the binding site of linezolid (pink) on D50S (*A*) with chloramphenicol (PDB ID code 1K01; green) (6) (*B*), anisomycin (PDB ID code 1K73; olive) (3) (*C*), tiamulin (PDB ID code 1XBP; teal) (7) (*D*), clindamycin (PDB ID code 1JZX; magenta) (6) (*E*), and A- (yellow) and P-site (orange) phenylalanyl-tRNA CCA-end mimics (PDB ID code 1VQN) (27) (*F*). In all cases, U2585 (blue) from the D50S-linezolid structure is shown for reference.

Linezolid Binds at the Ribosomal A Site. Most of the mutations that confer resistance to linezolid are also associated with resistance to a variety of other antibiotics that bind at the PTC, such as anisomycin, chloramphenicol, and the pleuromutilin class of drugs (tiamulin) (Fig. 1*A*). Consistently, a comparison of the structures of these antibiotics bound to the ribosome reveals a significant overlap in the binding site with linezolid, mostly with the oxazolidinone ring, and to a lesser extent with the central ring-B (Fig. 4 *A–E*). This finding is in agreement with an earlier observation that linezolid competes with chloramphenicol and lincomycin for binding to the ribosome (31). Indeed, alignment of the *H. marismortui* 50S subunit bound with phenylalanyl-tRNA CCA-end mimics (27) reveals that linezolid clearly overlaps with the position of the aminoacyl moiety in the A site (Fig. 4*F*). Thus, it is unclear why in some systems oxazolidinones have little inhibitory effect on fMet-puromycin formation (23, 31, 32), whereas in others an obvious effect is observed (15, 20, 22). Because the drug does not encroach on the P site (Fig. 4*F*), we suggest that the differential effects that oxazolidinones have on fMet-tRNA binding at the P site (11, 19, 22, 32) are probably indirect and related to the nonproductive drug-induced conformation of nucleotides within the PTC, such as U2585 and U2506.

Discussion

We have used x-ray crystallography to elucidate the binding site of the oxazolidinone linezolid on the *D. radiodurans* large ribosomal subunit. The drug is located in the A site pocket at the PTC of the ribosome (Fig. 4*A*), overlaps significantly with the aminoacyl moiety of an A site bound tRNA (Fig. 4*F*), and stabilizes a distinct conformation of nucleotide U2585 (Fig. 3*A*). In conjunction with available biochemical data, these findings allow us to propose a model for the mechanism of oxazolidinone action (Fig. 5).

After translation initiation, the ribosome is programmed with an initiator-tRNA at the P site inducing a distinct conformation of U2585 (Fig. 5*A*, Pi state) (27). The aminoacyl-tRNA is delivered to the A site in the form of a ternary complex with EF-Tu and GTP, initially binding at the A/T state (Fig. 5*B*) and then accommodating into the A/A site (Fig. 5*C*, red arrow) (33) to form a pretranslocational (PRE) state i.e., tRNAs at A and P sites (Fig. 5*C*). Peptide bond formation transfers the nascent chain to the A-tRNA and subsequently, EF-G catalyzes the translocation of the tRNAs from PRE to posttranslocational (POST) state i.e., tRNAs at P and E sites (Fig. 5*D*). Linezolid can bind to the free A site of an empty 50S subunit (31) or Pi state ribosome (15, 20) and stabilize U2585 in a nonproductive conformation (Fig. 5*E*). Because U2585 is required for the correct positioning of the P-tRNA (28), the presence of linezolid indirectly affects binding and/or positioning of the initiator-tRNA at the P site (22), but does not interfere with binding of the ternary complex (Fig. 5*F*) (11). After GTP hydrolysis and release of EF-Tu, however, the tRNA cannot fully accommodate into the A site on the PTC because the position is blocked by linezolid (Fig. 5*G*) and will therefore dissociate from the ribosome, analogous to the situation with tetracycline (Fig. 5*H*) (33). At this stage, the P-site still retains a peptidyl moiety, the ribosome is considered "locked" and thus is not a substrate for EF-G (36) (Fig. 5*H*). The loss of tRNA at the A site during elongation leaves only a single tRNA at the P site, which is known to be unstable in some cases and lead to framshifting (reviewed in ref. 34), as observed in the presence of linezolid (21, 35).

In vivo cross-linking studies have revealed that various oxazolidinone derivatives cross-link not only to 23S rRNA nucleotides within the PTC and a small RNA species the size of tRNA, but

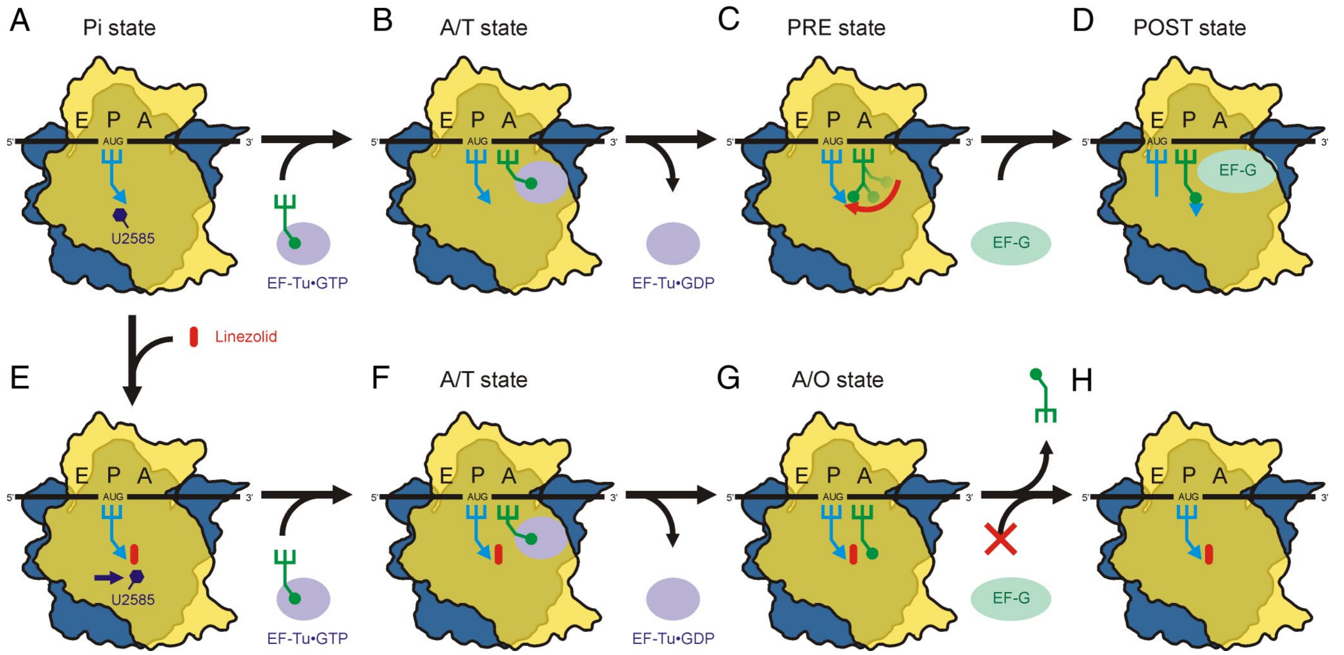

Fig. 5. Model for the inhibitory action of oxazolidinones during translation. Model showing events during normal translation (*A–D*), compared with the effect of the oxazolidinone linezolid (red) during translation (*E–H*), as described in the text. Small and large subunits are shown in yellow (transparent) and blue, respectively.

also to the ribosomal elongation factor LepA (12, 13). LepA is a translational GTPase that binds to POST state ribosomes inducing a back-translocation to the PRE state (37). We recently determined a cryo-electron microscopy reconstruction of LepA trapped in the process of back-translocating tRNAs by using the nonhydrolyzable GTP analogue GDPNP (50). This structure reveals that LepA does not simply reverse the EF-G mediated translocation process, but operates through a pre-A site accommodation intermediate (termed A/L state). In fact, the tRNA position is reminiscent of an intermediate observed during the simulation of an tRNA accommodating into the A site of the PTC after being released from EF-Tu (Fig. S5*a*) (38). Consistently, although the position of linezolid overlaps the A site in the PTC, the position of the LepA bound tRNA (A/L state) is compatible with the simultaneous presence of the drug (Fig. S5*a*). In the context of our model, this finding would suggest that LepA may recognize and bind to the functional state induced by the oxazolidinone i.e., an A/O state and via back-translocation of the tRNA attempt to rescue the stalled ribosome, consistent with the proposed role of this protein during elongation under stress conditions (Fig. S5*b*) (37). In this regard, we note however that a Δ*lepA* strain has an identical IC_{50} for oxazolidinones as the wild-type strain (12), suggesting that the binding of LepA is a consequence, rather than a cause, of the functional state induced by the oxazolidinones.

In conclusion, this study provides a definitive visualization of the linezolid binding mode and reveals the conformation of the PTC induced by the presence of the drug. It will be interesting to determine the structure of various oxazolidinone derivatives on the ribosome in the presence of peptidyl-tRNA CCA-ends mimicking initiator and/or elongator tRNAs. Such studies will provide not only better understanding of the mechanism of action of the oxazolidinones but also valuable insight into potential avenues toward rational drug development.

Experimental Procedures

Crystallography. *D. radiodurans* large ribosomal subunit crystals were prepared as previously described (6) and soaked in a cryo-solution containing 5 μM linezolid for 2 h before freezing. Data to 3.3 Å were collected at 100 K from shock-frozen crystals at X06SA at Swiss Light Source (SLS; Villigen, Switzerland). Data were recorded on a MAR345 CCD detector and processed with HKL2000 (40) and the CCP4 package (41).

Modeling and Docking:. The native structure of the D50S subunit [Protein Data Bank (PDB) ID code 2ZJR] (42) was refined against the structure factor amplitudes of the D50S-linezolid complex by using rigid body refinement as implemented in CNS (43). Initial refinement and map-calculation included data up to 3.3 Å, which were restricted to 3.5 Å in the final stage because of inferior completeness (73%) in the highest resolution bin. For the calculation of the free *R* factor, 5% of the data were omitted during refinement. The position of the drug was determined from σ-weighted difference maps or composite omit maps followed by density modification and phase recombination as described in (44). Further refinement was carried out by using CNS (see Table S1 for refinement statistics). Initially, the small molecule structure of linezolid from the *E. coli* 70S-linezolid model was used (13), whereas structures of other oxazolidinone derivatives were generated by using CORINA and ChemSketch. Comparison of the various ribosome crystal structures was performed by least square alignments onto the D50S structure by using the backbone atoms within 20 Å of the linezolid drug.

Coordinates and Figures. All crystallographic figures were produced using PyMol (http://www.pymol.org). Final coordinates and structure factors for linezolid-D50S have been deposited in the Protein Data Bank (ID code 3DLL).

ACKNOWLEDGMENTS. We thank Dr. Francois Franceschi for providing the linezolid compound; Drs. Alexander Mankin and James Blinn for the coordinates of the *E. coli* 70S-linezolid model and small-molecule structures of related oxazolidinone compounds; and the staff at the synchrotron facilities X06SA/SLS, in particular Dr. Takashi Tomazaki and Dr. Clemens Schulze-Briese, for expert assistance. This work was supported by the Deutsche Forschungsgemeinschaft Grants FU579 1-3 (to P.F.) and WI3285/1-1 (to D.N.W.). P.F. was supported by the Cluster of Excellence ''Macromolecular Complexes'' at the Goethe University Frankfurt (DFG Project EXC 115).

1. Spahn CMT, Prescott CD (1996) Throwing a spanner in the works: Antibiotics and the translational apparatus. *J Mol Med* 74:423–439.
2. Wilson DN (2004) in *Protein Synthesis and Ribosome Structure*, eds Nierhaus K, Wilson DN (Wiley–VCH, Weinheim), pp 449–527.
3. Hansen JL, Moore PB, Steitz TA (2003) Structures of five antibiotics bound at the peptidyl transferase center of the large ribosomal subunit. *J Mol Biol* 330:1061–1075.
4. Harms J, *et al.* (2004) Alterations at the peptidyl transferase centre of the ribosome induced by the synergistic action of the streptogramins dalfopristin and quinupristin. *BMC Biol* 2:4.
5. Tu D, Blaha G, Moore P, Steitz T (2005) Structures of MLSBK antibiotics bound to mutated large ribosomal subunits provide a structural explanation for resistance. *Cell* 121:257–270.
6. Schlünzen F, *et al.* (2001) Structural basis for the interaction of antibiotics with the peptidyl transferase centre in eubacteria. *Nature* 413:814–821.
7. Schlunzen F, *et al.* (2004) Inhibition of peptide bond formation by pleuromutilins: The structure of the 50S ribosomal subunit from Deinococcus radiodurans in complex with tiamulin. *Mol Microbiol* 54:1287–1294.
8. Vara Prasad J (2007) New oxazolidinones. *Curr Opin Microbiol* 10:454–460.
9. Hutchinson DK (2004) Recent advances in oxazolidinone antibacterial agent research. *Expert Opin Ther Pat* 14:1309–1328.
10. Bozdogan B, Appelbaum P (2004) Oxazolidinones: Activity, mode of action, and mechanism of resistance. *Int J Antimicrob Agents* 23:113–119.
11. Matassova NB, *et al.* (1999) Ribosomal RNA is the target for oxazolidinones, a novel class of translational inhibitors. *RNA* 5:939–946.
12. Colca JR, *et al.* (2003) Crosslinking in the living cell locates the site of action of oxazolidinone antibiotics. *J Biol Chem* 278:21972–21979.
13. Leach KL, *et al.* (2007) The site of action of oxazolidinone antibiotics in living bacteria and in human mitochondria. *Mol Cell* 26:393–402.
14. Kloss P, Xiong L, Shinabarger DL, Mankin AS (1999) Resistance mutations in 23 S rRNA identify the site of action of the protein synthesis inhibitor linezolid in the ribosomal peptidyl transferase center. *J Mol Biol* 294:93–101.
15. Sander P, *et al.* (2002) Ribosomal and non-ribosomal resistance to oxazolidinones: Species-specific idiosyncrasy of ribosomal alterations. *Mol Microbiol* 46:1295–1304.
16. Xiong L, *et al.* (2000) Oxazolidinone resistance mutations in 23S rRNA of Escherichia coli reveal the central region of domain V as the primary site of drug action. *J Bacteriol* 182:5325–5331.
17. Tsiodras S, *et al.* (2001) Linezolid resistance in a clinical isolate of. Staphylococcus aureus. *Lancet* 358:207–208.
18. Prystowsky J, *et al.* (2001) Resistance to linezolid: characterization of mutations in rRNA and comparison of their occurrences in vancomycin-resistant enterococci. *Antimicrob Agents Chemother* 45:2154–2156.
19. Swaney SM, Aoki H, Ganoza MC, Shinabarger DL (1998) The oxazolidinone linezolid inhibits initiation of protein synthesis in bacteria. *Antimicrob Agents Chemother* 42:3251–3255.
20. Burghardt H, Schimz KL, Muller M (1998) On the target of a novel class of antibiotics, oxazolidinones, active against multidrug-resistant Gram-positive bacteria. *FEBS Lett* 425:40–44.
21. Thompson J, O'Connor M, Mills JA, Dahlberg AE (2002) The protein synthesis inhibitors, oxazolidinones and chloramphenicol, cause extensive translational inaccuracy. *in vivo J Mol Biol* 322:273–279.
22. Aoki H, *et al.* (2002) Oxazolidinone antibiotics target the P site on Escherichia coli ribosomes. *Antimicrob Agents Chemother* 46:1080–1085.
23. Shinabarger DL, *et al.* (1997) Mechanism of action of oxazolidinones: effects of linezolid and eperezolid on translation reactions. *Antimicrob Agents Chemother* 41:2132–2136.
24. Schuwirth B, *et al.* (2005) Structures of the bacterial ribosome at 3.5 Å resolution. *Science* 310:827–834.
25. Klein D, Moore P, Steitz T (2004) The roles of ribosomal proteins in the structure assembly, and evolution of the large ribosomal subunit. *J Mol Biol* 340:141–177.
26. Selmer M, *et al.* (2006) Structure of the 70S ribosome complexed with mRNA and tRNA. *Science* 313:1935–1942.
27. Schmeing TM, Huang KS, Strobel SA, Steitz TA (2005) An induced-fit mechanism to promote peptide bond formation and exclude hydrolysis of peptidyl-tRNA. *Nature* 438:520–524.
28. Green R, Samaha RR, Noller HF (1997) Mutations at nucleotides G2251 and U2585 of 23 S rRNA perturb the peptidyl transferase center of the ribosome. *J Mol Biol* 266:40–50.
29. Youngman EM, Brunelle JL, Kochaniak AB, Green R (2004) The active site of the ribosome is composed of two layers of conserved nucleotides with distinct roles in peptide bond formation and peptide release. *Cell* 117:589–599.
30. Gale EF, *et al.* (1981) in *The molecular basis of antibiotic action* (Wiley, Bristol, U.K.), pp 278–379.
31. Lin AH, Murray RW, Vidmar TJ, Marotti KR (1997) The oxazolidinone eperezolid binds to the 50S ribosomal subunit and competes with binding of chloramphenicol and lincomycin. *Antimicrob Agents Chemother* 41:2127–2131.
32. Eustice DC, Feldman PA, Zajac I, Slee AM (1988) Mechanism of action of DuP 721: Inhibition of an early event during initiation of protein synthesis. *Antimicrob Agents Chemother* 32:1218–1222.
33. Blanchard SC, *et al.* (2004) tRNA selection and kinetic proofreading in translation. *Nat Struct Mol Biol* 11:1008–1014.
34. Wilson DN, Nierhaus KH (2006) The E-site Story: The importance of maintaining two tRNAs on the ribosome during protein synthesis. *Cell Mol Life Sci* 63:2725–2737.
35. Thompson J, Pratt CA, Dahlberg AE (2004) Effects of a number of classes of 50S inhibitors on stop codon readthrough during protein synthesis. *Antimicrob Agents Chemother* 48:4889–4891.
36. Zavialov AV, Ehrenberg M (2003) Peptidyl-tRNA regulates the GTPase activity of translational factors. *Cell* 114:113–122.
37. Qin Y, *et al.* (2006) The highly conserved LepA is a ribosomal elongation factor that back-translocates the ribosome. *Cell* 127:721–733.
38. Sanbonmatsu KY, Joseph S, Tung CS (2005) Simulating movement of tRNA into the ribosome during decoding. *Proc Natl Acad Sci USA* 102:15854–15859.
39. Eustice DC, Feldman PA, Slee AM (1988) The mechanism of action of DuP 721, a new antibacterial agent: Effects on macromolecular synthesis. *Biochem Biophys Res Commun* 150:965–971.
40. Otwinowski Z, Minor W (1997) Processing of X-ray diffraction data collected in oscillation mode. *Methods Enzymol* 276:307–326.
41. Bailey S (1994) The CCP4 suite: Programs for protein crystallography Collaborative Computational Project, Number 4. *Acta Crystallogr D* 50:760–763.
42. Wilson D, *et al.* (2005) Species-specific antibiotic-ribosome interactions: Implications for drug development. *Biol Chem* 386:1239–1252.
43. Brunger A, *et al.* (1998) Crystallography & NMR system: A new software suite for macromolecular structure determination. *Acta Crystallogr D* 54:905–921.
44. Diaconu M, *et al.* (2005) Structural basis for the function of the ribosomal L7/12 stalk in factor binding and GTPase activation. *Cell* 121:991–1004.
45. Mankin AS, Garrett RA (1991) Chloramphenicol resistance mutations in the single 23S rRNA gene of the archaeon Halobacterium halobium. *J Bacteriol* 173:3559–3563.
46. Gregory ST, Carr JF, Rodriguez-Correa D, Dahlberg AE (2005) Mutational analysis of 16S and 23S rRNA genes of Thermus thermophilus. *J Bacteriol* 187:4804–4812.
47. Hummel H, Boeck A (1987) 23S ribosomal RNA mutations in halobacteria conferring resistance to the anti-80 S ribosome targeted antibiotic anisomycin. *Nucleic Acids Res* 15:2431–2443.
48. Blaha G, *et al.* (2008) Mutations outside the anisomycin binding site can make ribosomes drug-resistant. *J Mol Biol* 379:505–519.
49. Pringle M, Poehlsgaard J, Vester B, Long KS (2004) Mutations in ribosomal protein L3 and 23S ribosomal RNA at the peptidyl transferase centre are associated with reduced susceptibility to tiamulin in Brachyspira spp. isolates. *Mol Microbiol* 54:1295–1306.
50. Connell SR, *et al.* (2008) A new tRNA intermediate revealed on the ribosome during EF4-mediated back-translocation. *Nat Struct Mol Biol*, in press.